

# CDistNet: Perceiving Multi-Domain Character Distance for Robust Text Recognition

Tianlun Zheng<sup>1</sup> Zhineng Chen<sup>1\*</sup> Shancheng Fang<sup>2</sup> Hongtao Xie<sup>2</sup> Yu-Gang Jiang<sup>1</sup>

<sup>1</sup>Fudan University

<sup>2</sup>University of Science and Technology of China

tlzheng21@m.fudan.edu.cn, {zhinchen, ygj}@fudan.edu.cn, {fangsc, htxie}@ustc.edu.cn

## Abstract

The attention-based encoder-decoder framework is becoming popular in scene text recognition, largely due to its superiority in integrating recognition clues from both visual and semantic domains. However, recent studies show the two clues might be misaligned in the difficult text (e.g., with rare text shapes) and introduce constraints such as character position to alleviate the problem. Despite certain success, a content-free positional embedding hardly associates with meaningful local image regions stably. In this paper, we propose a novel module called Multi-Domain Character Distance Perception (MDCDP) to establish a visual and semantic related position encoding. MDCDP uses positional embedding to query both visual and semantic features following the attention mechanism. It naturally encodes the positional clue, which describes both visual and semantic distances among characters. We develop a novel architecture named CDistNet that stacks MDCDP several times to guide precise distance modeling. Thus, the visual-semantic alignment is well built even various difficulties presented. We apply CDistNet to two augmented datasets and six public benchmarks. The experiments demonstrate that CDistNet achieves state-of-the-art recognition accuracy. While the visualization also shows that CDistNet achieves proper attention localization in both visual and semantic domains. The code will be released in <https://github.com/simplify23/CDistNet>.

## 1. Introduction

Scene text recognition aims to read text in natural images. It has attracted increasing interest due to its pivotal role in extracting high-level textual information that is critical for many vision-related applications. Despite extensive studies [1, 6, 15, 30] carried out over the years, the task still remains challenging for several difficulties, e.g., complex text deformations, unequally distributed characters, cluttered background, etc. How to tackle these challenges is becoming a key issue for modern text recognizers.

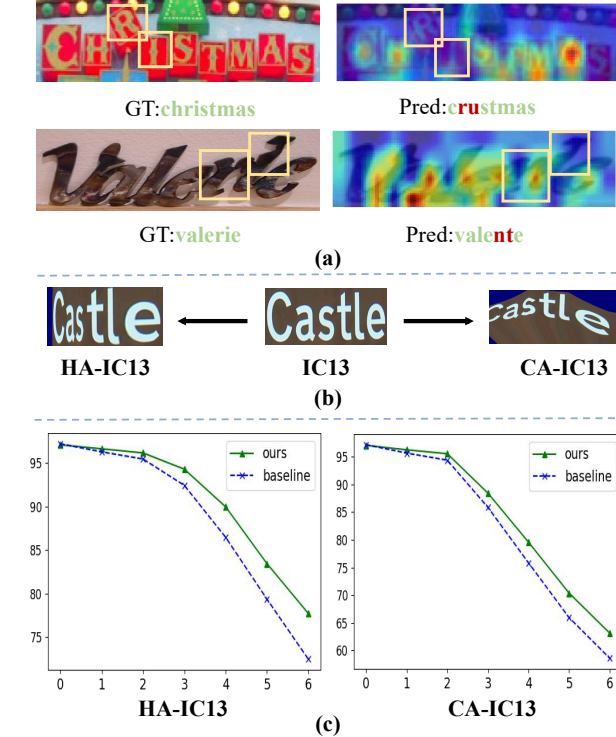


Figure 1. (a) Traditional attention-based encoder-decoder recognizer [6, 29, 37, 43] encounters the *attention drift* problem and gets incorrect results. (b) HA-IC13 and CA-IC13 datasets are created by horizontal and curved stretching ICDAR2013 with various scales. (c) We develop CDistNet that perceives multi-domain character distance better by position-related joint encoding. Compared with baseline, the accuracy margin becomes larger as the deformation severity rises.

Recently, attention-based encoder-decoder methods attain impressive performance in this task. Lee *et al.* [15] extracts visual feature from the text image, and encodes semantic feature from the annotations on the encoder side.

During decoding, the text image is identified character-by-character. At each time step, the semantic feature is used as the *query* vector to align its correspondence in the visual space, by which the two kinds of features are fused and a character-level recognition decision is derived. The pipeline [1, 27, 29] has advantages such as providing a unified way of integrating recognition clues from both visual and semantic domains. However, recent studies [38] show the two clues are easily mismatched in rare irregular text, as the two incorrectly recognized examples in Fig.1 (a). It is explained as when the visual clue is weak, the semantic clue could not stably find its visual counterpart. Moreover, it is also shown in [38, 44] that the mismatch is more prevalent in long text, where the semantic feature is gradually reinforced and dominates the recognition as the accumulation of decoded characters. The two phenomena are roughly summarized as *attention drift* in the literature [3, 19, 35].

In view of the problem above, several studies utilize the character position to alleviate the mismatch, where the information is encoded as sinusoidal-like positional embedding [6, 29] or others [35, 43, 44]. Despite tackling the problem to some extent, these works [29, 44] employ a content-free positional embedding to interact with the visual feature and hardly establish a stable association between character positions and local image regions. It is more like a position order constraint rather than a content-aware receptor. Besides, they also ignore mining relationships between the position and semantic space. Therefore, the performance gain is limited.

In this paper, we develop a novel module called *Multi-Domain Character Distance Perception* (MDCDP) to overcome the aforementioned issues. Similar to existing studies [34, 44], a fixed positional embedding is initialized. But differently, the feature from encoder first experiences a self-attention enhancement and then be used as the *query* vector to interact with both visual and semantic features following the attention mechanism. It imposes positional enhancement to both domains. The results of the two enhanced features can be viewed as a visual and semantic distance-aware representation. It encodes the relationship among characters in both domains. The previous position feature is used as query vector to the next MDCDP, a more attention-focused visual-semantic alignment can be obtained. Following this idea, we propose a novel architecture named CDistNet that stacks MDCDP several times to guide precise distance modeling, which is beneficial to the recognition even complex character spatial layouts presented.

To evaluate CDistNet, we augment the ICDAR2013 dataset by horizontal and curved stretching of multiple scales and create two challenging datasets termed HA-IC13 and CA-IC13 (as illustrated in Fig.1 (b)). It is seen in Fig.1 (c) that CDistNet attains larger accuracy margin as the deformation severity rises when compared with a

Transformer-based baseline, showing its effectiveness in handling difficult text. Moreover, we also apply CDistNet to six popular regular and irregular text benchmarks and compare it with existing methods. It achieves state-of-the-art recognition accuracy among the competitors. We also visualize the attention map and semantic affinities among the characters during decoding. It is shown that proper attention localization in both visual and semantic domains are obtained, which explains the accuracy gains.

The contribution of this paper is threefold. First, we propose MDCDP that employs the positional feature to query both visual and semantic features. It enables visual and semantic distance-aware position modeling for the first time, generating superior attention-focused visual-semantic alignment. Second, we develop a novel text recognizer termed CDistNet. It stacks several MDCDP to well perceive the character distance, benefiting recognizing difficult text. Third, we carry out extensive experiments with different configurations and compare CDistNet with existing methods. It achieves state-of-the-art recognition accuracy while the visualization implies CDistNet achieves proper attention localization in both visual and semantic domains.

## 2. Related Work

Recently, most research efforts in scene text recognition [1, 4, 20, 25, 30] are devoted to irregular text while sequence-based methods [2, 22, 32] have been popular, as different recognition clues (e.g., visual, semantic) are jointly modeled to get the prediction. Based on how these clues are utilized, we can broadly categorize them into semantic-free, semantic-enhanced, and position-enhanced methods.

### 2.1. Semantic-free Methods

They implement the recognition by utilizing image visual features mainly, while the semantic relationship among characters is not explicitly modeled. For example, Shi *et al.* [30] proposed the CTC-based method, where the visual feature extracted by CNN was reshaped as a sequence and then modeled by RNN and CTC loss. Following this pipeline, several methods were developed with improved accuracy [8, 9, 33]. Rather than decoding by RNN, segmentation-based methods [17, 19, 40] directly performed pixel-level character segmentation and prediction. However, they generally required character-level annotations which were not always readily available. Moreover, the performance of these methods was limited, due to not well modeling the semantic clue.

### 2.2. Semantic-Enhanced Methods

They emphasize leveraging the semantic clue to reinforce the visual feature and always using the encoder-decoder with attention framework. Lee *et al.* [15] first introduced the attention mechanism into the scene text recog-

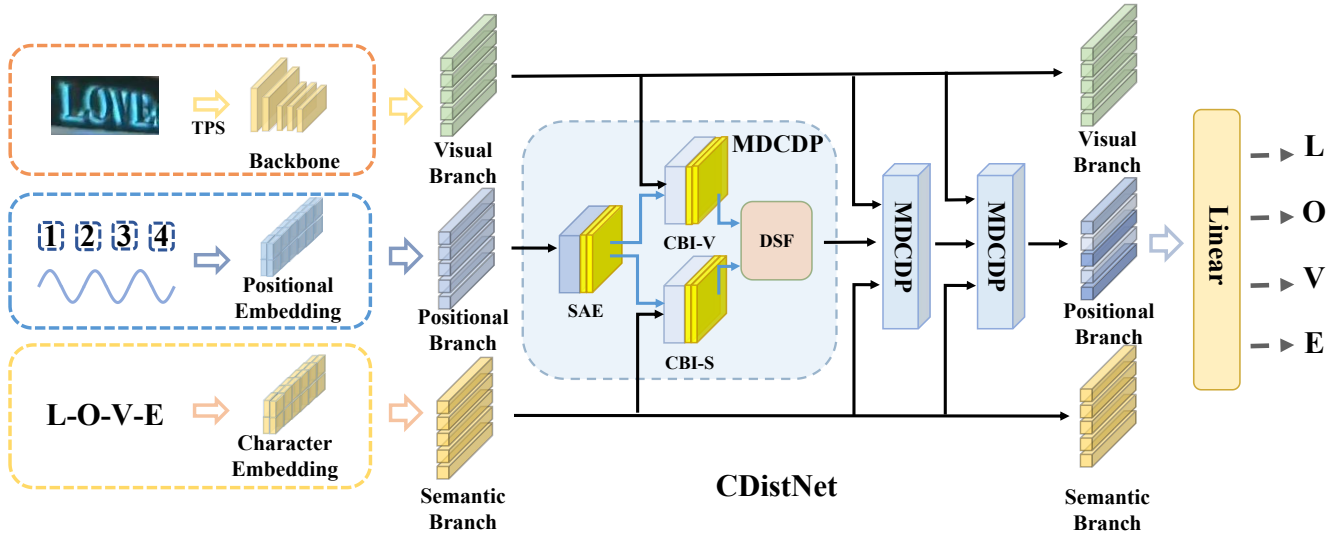


Figure 2. A schematic overview of the proposed CDistNet. The encoder consists of the visual, semantic, and positional branches. The three kinds of features are fed into the *Multi-Domain Character Distance Perception* (MDCDP) module that learns a visual and semantic distance-aware representation. SAE, CBI and DSF are proposed blocks which will be elaborated later. Output of the last MDCDP is leveraged to decode the characters sequentially.

nition. It employed the 1D image feature and embedding of the character sequence, by which the semantic information was considered. Then, it was extended by designing a more natural 2D image feature [16], adding dedicated attention enhancement modules [3], etc. By substituting RNN with Transformer [34], a powerful model in capturing global spatial dependence, many variants [23, 29, 37] were developed with improved accuracy. Several Transformer-based efforts were conducted by introducing semantic loss of different forms [6, 27, 39]. Fang *et al.* [6] presented a novel language model to guide semantic information utilization and got impressive results. Despite great processes made, it was observed that there were misalignment between characters and local image regions especially in long text, i.e., *attention drift* [3, 19, 35].

### 2.3. Position-Enhanced Methods

They develop a dedicated character position encoding to ease the recognition. Early work such as RARE [31] employed STN [11] to rectify the text before feeding it into the recognition network. It is an early form of utilizing the position clue. Although advanced rectification models were developed [32, 42, 45], a rectification in isolation could not evoke a synergistic utilization of different clues.

On the other hand, positional encoding was commonly applied to Transformer-based models whose attention mechanism was non-local. For example, sinusoidal positional embedding was employed to record the character position in [29]. Noticing that the embedding is fixed, learnable embedding was also developed to adaptively utilize the

position information in [5, 14]. To suppress *attention drift*, TextScanner [35] proposed an order segmentation map to ensure that characters were read in the right order and separated properly. Meanwhile, RobustScanner [44] proposed a position enhancement branch along with a dynamical fusion mechanism and achieved impressive results. Our work also falls into this category. However, different with [44] used a content-free positional embedding that hardly built a stable correspondence between positions and local image regions, we inject the positional embedding to both visual and semantic features andto establish a multi-domain distance-aware modeling, which eases the recognition of difficult text.

## 3. Methodology

The proposed CDistNet is given in Fig.2. It is an end-to-end trainable network falling into the attention-based encoder-decoder framework. Specifically, the encoder consists of three branches, respectively for encoding visual, positional and semantic information. On the decoder side, the three kinds of information are fused by a dedicated designed MDCDP module, in which the positional branch is leveraged to reinforce both visual and semantic branches and generate a new hybrid distance-aware positional embedding. The generated embedding, which records the relationship among characters in both visual and semantic domains, is used as the positional embedding of the next MD-CDP. It is thus conducive to generating a attention-focused visual-semantic alignment. The MDCDP module is stacked several times in CDistNet to achieve a more precise dis-

tance modeling. At last, characters are decoded sequentially based on the output of the last MDCDP module.

### 3.1. Encoder

**Visual Branch.** The visual branch utilizes Thin-plate-splines (TPS) as a preprocess to rectify the text images [1, 32]. Then, similar to [6, 43], ResNet-45 and Transformer units are applied as backbone in Fig.2, which captures both local and global spatial dependencies. The same ResNet-45 as [32, 38] is used. Besides, the Transformer units are three-layer self-attention encoders with 1024 hidden units per layer. The process can be described using the following formula.

$$\mathbf{F}_{vis} = \tau(\mathcal{R}(\mathbb{T}(I))) \in \mathbb{R}^{\frac{HW}{64} \times C} \quad (1)$$

where  $I$  denotes the input text image,  $\mathbb{T}$  is the TPS block.  $\mathcal{R}$  represents ResNet-45 and  $\tau$  is the Transformer unit. ResNet-45 downsamples both the width and height to 1/8 of the original size.

**Semantic Branch.** Similar to [29, 44], the semantic branch encodes previously seen characters during training. While in the test phase, previously decoded characters are encoded as current semantic feature which is updated at each time step. Embedding of the start token is used when decoding the first character.

**Positional Branch.** As an initial, the positional branch encodes the character position in the text. Given a character position, we first generate a one-hot vector that "1" appears in the corresponding dimension while "0" otherwise. Then, we use the same sinusoidal positional embedding as in [34] to get the embedding.

### 3.2. MDCDP

We then explain how the MDCDP module is formulated on the decoder side and benefit the recognition. MDCDP consists of three parts, a self-attention enhancement for positional feature reinforcement, a cross-branch interaction that utilizes positional feature to *query* both the visual and semantic branches, obtaining positional-enhanced representations, and a dynamic shared fusion to get a visual and semantic joint embedding. As a result, the three features are fused and a distance-aware representation is obtained.

**Self-Attention Enhancement (SAE).** With the initial positional embedding from the encoder, SAE reinforces the embedding using one multi-head self-attention block from the vanilla Transformer [34] but half its dimension to reduce the computational cost. In addition, as shown in Fig.3 (a), an upper triangular mask is applied to the query vector of the self-attention block to prevent from "seeing itself", or saying, leaking information across time steps.

Note that RobustScanner [44] does not set such a enhancement before using the positional embedding to *query*

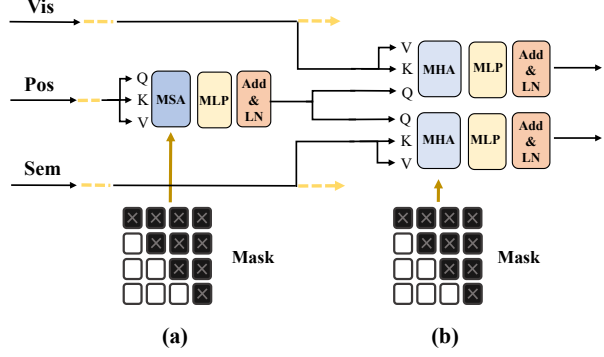


Figure 3. Detail structures of (a) Self-Attention Enhancement (SAE) and (b) Cross-Branch Interaction (CBI).

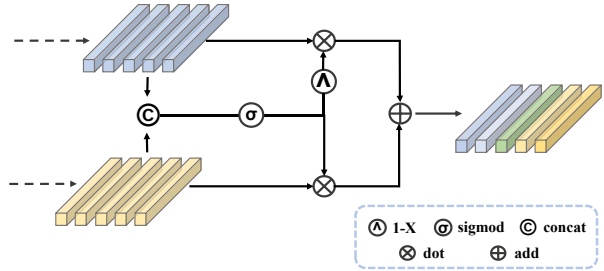


Figure 4. Detail structure of Dynamic Shared Fusion (DSF).

the visual feature. The query vector is always fixed in different character sequences. As a contrast, our enhancement enables a more targeted positional embedding learning.

**Cross-Branch Interaction (CBI).** As depicted in Fig.3 (b), the enhanced positional embedding is treated as the query vector and fed into the visual and semantic branches in parallel. When applying to the visual branch, it uses previous decoded character locations to search the position of the next character in the text image. The sub-branch is termed as CBI-V. While applying to the semantic branch, it models the semantic affinities between previous decoded characters and current positional clue. The sub-branch is termed as CBI-S. Both branches have been reinforced after the interactions. A similar upper triangular mask is also applied to the semantic branch to prevent information leaks due to its dynamical update nature.

Note that previous studies [1, 16] use the semantic feature as the query to interact with the visual feature. RobustScanner [44] extends it by adding an additional query from position to visual and enables a positional-enhanced decoding. However, it leaves the semantic branch untouched. In contrast, we formulate the interactions as the positional-based intermediate enhancement to both visual and semantic domains. It reinforces not only visual but also semantic features and can be understood as delineating the multi-domain character distance.

**Dynamic Shared Fusion (DSF).** As depicted in Fig.4, DSF

takes the two positional-enhanced features as input. They are concatenated to a hybrid feature whose channels are doubled. Then, the feature undergoes a  $1 \times 1$  convolution that halves the channels, i.e., retaining the same size as either input feature. After that, a gating mechanism is designed to transform it to weight matrices, which are applied to both visual and semantic features element-wisely, forming a dynamic fusion of features across visual and semantic domains. Formally,

$$\hat{\mathbf{F}} = \sigma([\mathbf{F}_{sem}, \mathbf{F}_{vis}]\mathbf{W}_{conv}) \quad (2)$$

$$\mathbf{F}_{out} = \hat{\mathbf{F}} \otimes \mathbf{F}_{sem} + (1 - \hat{\mathbf{F}}) \otimes \mathbf{F}_{vis} \quad (3)$$

where  $\mathbf{F}_{sem}$  and  $\mathbf{F}_{vis}$  indicate the positional-enhanced semantic and visual features, respectively.  $\mathbf{W}_{conv} \in \mathbb{R}^{2C \times C}$  denotes the convolution. Note that the fusion is efficient while similar operations are also considered in [6, 43, 44].

One peculiarity of DSF is that the weights are shared among different MDCDP modules. As a consequence, DSF not only decouples the feature fusion with the previous attention learning, but also eases the network modeling. We verify its effectiveness in ablation study.

## 4. Experiments

### 4.1. Datasets

Our work is related to three kinds of datasets, i.e., two synthetic datasets for model training, two augmented datasets for model verification, and six widely used public datasets for both ablation study and comparison with existing methods. They are described as follows.

**MJSynth (MJ)** [10] and **SynthText (ST)** [7] are two synthetic datasets each with millions of text images. Nearly 8.91M text instances from MJ and 6.95M from ST are retained for model training.

**HA-IC13** and **CA-IC13** are two augmented datasets created from ICDAR2013. They simulate the horizontal (HA-IC13) and curved (CA-IC13) stretching with scales from 1 (the smallest deformation) to 6 (the largest deformation) with interval of 1 using the data augmentation tool in [21]. Certain postprocessing is applied to handle the exception that the character exceeds the boundary of the image. Both datasets are augmented counterparts of ICDAR2013 and their image numbers are six times to the raw dataset. Examples of the two datasets are shown in Fig.5.

**ICDAR2013 (IC13)** [13], **Street View Text (SVT)** [36], **IIIT5k-Words (IIIT5k)** [24], **ICDAR2015 (IC15)** [12], **SVT-Perspective (SVTP)** [26] and **CUTE80 (CUTE)** [28] are six standard benchmarks. The first three mainly contain regular text while the rest three are irregular. Configurations of the datasets can refer to [1].

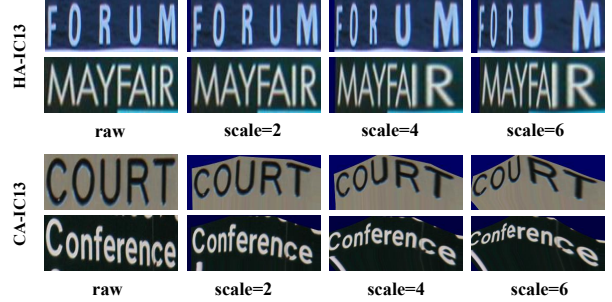


Figure 5. Augmented text images in HA-IC13 (top) and CA-IC13 (bottom), which simulate horizontal and curved stretching of varying scales, respectively.

### 4.2. Implementation details

We resize the input images to  $32 \times 128$  and employ data augmentation such as image quality deterioration, color jitter and geometry transformation. MJ and ST datasets are used for model training. While the two augmented datasets and the six public datasets are retained for model assessment at different scenarios. To train CDistNet, the initial learning rate is set to  $4 \times 10^{-4}$ . The first 10k iterations use warm-up strategy. The whole training iterations are determined by the following formula.

$$lr = d_{model}^{-0.5} \cdot \min(n^{-0.5}, n \cdot warm-up\_n^{-1.5}) \quad (4)$$

where  $n$  and  $warm-up\_n$  denote the number of normal iterations and warm-up iterations.  $d_{model}$  is set to 512. For ablation study and model verification, all models are trained for 6 epochs. When compared with existing methods, our model is trained 8 epochs following Eq.4 and then another 2 epochs with a constant learning rate of  $10^{-5}$ . The batch size is set to 700.

To reduce the computational cost, we shrink the transformer units employed, where dimension of the MLP layer is reduced from 2048 to 1024 in encoder, and from 2048 to 512 in decoder. The number of encoder and decoder layers are both set to 3. Beam search is applied to determine the decoded character sequence and its size is empirically set to 10. All experiments are conducted on a server with 6 NVIDIA 3080 GPUs using PyTorch platform.

### 4.3. Ablation study

To better understand CDistNet, we carry out controlled experiments on both SVT (regular text) and IC15 (irregular text) under different configurations as follows.

**The number of MDCDP modules considered.** Generally, stacking more MDCDP modules tends to generate comprehensive feature fusion, but increases computational cost. Ablation study on this point is given by Tab.1, where recognition accuracy and speed are both presented. The best accuracy is reported when three MDCDP modules are

#MDCDP	SVT	IC15	Speed (ms)
1	92.74	84.82	61.48
2	<b>94.28</b>	84.87	87.68
3	93.66	<b>85.92</b>	123.28
4	93.82	84.43	149.99

Table 1. Ablation study on the number of MDCDP modules.

equipped. It performs better than other cases where fewer (one and two) or more (four) modules are considered, while the increase in speed is also affordable. Therefore the MDCDP modules in CDistNet are empirically set to 3.

	Enhanced Branch			SVT	IC15
	Sem	Vis	Pos		
1	✓			92.89	84.70
2		✓		93.04	84.65
3	✓	✓		93.04	84.76
4			✓	<b>93.66</b>	<b>85.92</b>

Table 2. Ablation study on SAE, where Sem, Vis and Pos denotes the semantic, visual and positional branches, respectively.

**The effectiveness of SAE.** SAE injects positional learning ability to the positional branch, though there is no such block in [29, 43, 44]. Meanwhile, it is curious that further reinforcement of the visual and semantic features on the decoder side would benefit the recognition. With this doubt in mind, we apply SAE to different branches while Tab.2 gives the results. It is seen the differences are marginal when equipping SAE to either or both visual and semantic branches. Nevertheless, on positional branch the improvement is noticeable. The result is in accordance with our anticipation. The visual feature is extracted from a powerful hybrid backbone while the semantic feature is dynamically fortified during decoding. It is less meaningful to further reinforce them. In contrast, the positional feature comes from a fixed embedding while SAE is the only block for its self-adjustment. Therefore a larger improvement is observed.

	Interaction Pattern			SVT	IC15
	Sem_Vis	Pos_Vis	Pos_Sem		
1		✓		90.26	82.11
2	✓			91.34	84.04
3	✓		✓	92.27	85.37
4	✓	✓		92.89	84.93
5		✓	(✓)	93.35	84.70
6	✓	✓	✓	<b>93.66</b>	<b>85.92</b>

Table 3. Ablation study on CBI, where Sem\_Vis denotes using semantic feature to query visual feature. The others are similarly defined. (✓) means switching the roles of the two features.

**The effectiveness of CBI.** There are multiple ways to establish the CBI. We enumerate six of them and give the result in Tab.3. Our scheme (line 6) achieves the best result among the competitors. It is better than the scheme of Transformer [29, 34] (line 2) and RobustScanner [44] (line 4). The result basically validates two hypotheses. First, imposing the positional clue is helpful. Second, it is effective to query the semantic feature by using the positional clue, which perceives the semantic affinities between previous decoded characters and current position.

**The effectiveness of DSF.** We have tested four operations to fuse the positional-enhanced visual and semantic features. As shown in Tab.4, DSF outperforms static-based fusions (Add and Dot) as well as the scheme that not sharing weights among MDCDP modules.

Method	SVT	IC15
Add	91.96	85.48
Dot	91.81	84.21
DSF w/o WS [6]	93.51	85.04
<b>DSF</b>	<b>93.66</b>	<b>85.92</b>

Table 4. Ablation study on DSF, where WS denotes weight sharing among MDCDP modules.

#### 4.4. Model Verification

**Contribution of the positional utilization.** There are several methods encoding the positional information. However, CDistNet differs with them not only in the position utilization but also other aspects. To make a fair comparison, we modified the methods where other differences are mostly eliminated. The results are listed in Tab.5.

Method	SVT	IC15
CDistNet w/o Sem	90.26	82.11
Transformer* [29]	91.34 (-0.16)	84.04 ( <b>+5.00</b> )
RobustScanner* [44]	91.96 ( <b>+3.86</b> )	84.21 ( <b>+7.11</b> )
CDistNet (Ours)	<b>93.66</b>	<b>85.92</b>

Table 5. Quantitative comparison of different methods, where \* denotes our modified implementation. Values in bracket are accuracy improvements compared with the raw implementation.

We first explain how the methods are modified. *CDistNet w/o Sem* denotes the semantic branch is removed from CDistNet thus the positional feature only queries the visual feature (line 1 in Tab.3). In *Transformer\** (line 2 in Tab.3), we strengthen the raw implementation [29] using our visual encoding branch, from which 5 percents accuracy gain in IC15 is observed due to a superior encoder is equipped. Besides the visual encoder branch, *RobustScanner\** uses the

Transformer unit to replace the raw "CNN+LSTM" implementation. It improves the accuracy by 3.86 and 7.11 percents on SVT and IC15, respectively. Note that our modification leads to some improvements to the raw implementation.

With the modifications above, accuracy gains from the position modeling can be quantitatively evaluated. As can be seen, CDistNet still attains over 1.5 percents accuracy gains in both datasets compared with *RobustScanner\**, largely attributed to the character distance are perceived in both visual and semantic domains.

**Performance on augmented datasets.** As described, HA-IC13 and CA-IC13 are simulated with different levels of horizontal and curved deformations. It thus forms tested with gradual increased difficulties, a nearly ideal scenario for assessing CDistNet in recognizing difficult text.

We validate CDistNet in both datasets and Tab.6 presents the results, where *Transformer\** in Tab.5 is picked out as the baseline. Since the raw IC13 is relatively simple, the two methods both get quite high accuracy in the raw dataset. With the deformation scale rising, CDistNet gradually shows its superiority. It goes down slower, where accuracy margins of 5.25 and 4.55 percents are observed in the two datasets at scale 6, the most severe deformable case. It clearly verifies the advantage of CDistNet in recognizing difficult text.

Scale	HA-IC13		CA-IC13	
	Trans	CDistNet	Trans	CDistNet
0	97.2	97.1 (-0.10)	97.2	97.1(-0.10)
2	95.45	96.15 ( <b>+0.70</b> )	94.40	95.57 ( <b>+1.17</b> )
4	86.46	89.96 ( <b>+3.50</b> )	75.85	79.58 ( <b>+3.73</b> )
6	72.46	77.71 ( <b>+5.25</b> )	58.58	63.13( <b>+4.55</b> )

Table 6. Recognition accuracy of CDistNet and Transformer\* (Trans) on CA-IC13 and HA-IC13.

**Decoding Visualization.** We visualize the attention map based on the positional-enhanced visual branch and give some examples in Fig.6, where the text images and their attention maps are depicted. The characters are precisely localized on the attention map in most cases, attributed to the positional feature well encoding the spatial layout among characters. It again indicates the superiority of the proposed MDCDP module.

We also visualize the semantic affinities between previous decoded characters and current position in Fig.7, where three matrices, each corresponding to a specified method, are illustrated. In each matrix  $M$ , darker color indicates higher affinity value. Y-axis denotes the decoding time steps while X-axis represents the decoded characters. Thus,  $M(i, j)$  denotes when decoding the  $j$ th character, its position-semantic affinity with respect to the  $i$ th decoded

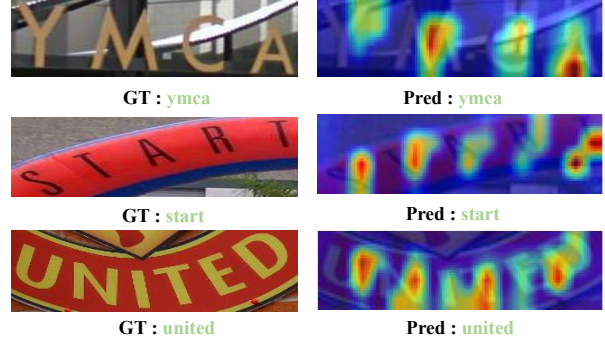


Figure 6. Attention map visualization of the positional-enhanced visual feature in the last MDCDP module.

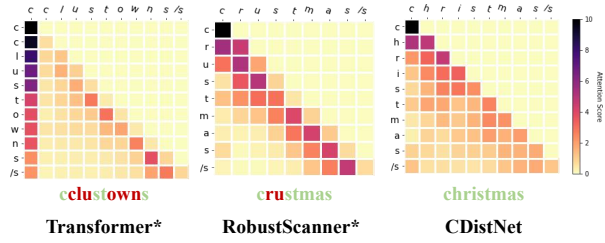


Figure 7. Semantic affinities visualization of the positional-enhanced semantic feature in the last MDCDP module when decoding "christmas". For the left and center ones, it denotes the semantic branches in our implemented [29] and [44], respectively.

character. As can be seen, for CDistNet the majority of previous decoded characters have darker color thus contributed to the decoding process. While for the other two methods, they mostly rely on the start token or nearby decoded characters. It demonstrates that the semantic distance is comprehensively modeled in CDistNet.

**Analysis of good and bad cases.** Some correctly recognized instances are given in Fig.8. From them we can conclude that CDistNet retains powerful and universal recognition capability with the existence of various difficulties, e.g., diverse text shapes, blur, distortions, etc. We also list some bad cases in Fig.9. The failures can be summarized as three categories mainly, multiple text fonts (cocacola, quilts), severe blur (coffee) and vertical text (garage). Most of them are even undistinguishable by humans and they are common challenges for modern text recognizers.

#### 4.5. Comparisons with Existing Methods

We compare CDistNet with eighteen existing methods published from year 2017 to 2021. It is shown that our CDistNet achieves the best results on five datasets including IC13, SVT, IIIT5K, IC15 and SVT-P when trained based on the two synthetic datasets. As expected, the performance gains are more prominent in irregular text datasets compared to regular text datasets, demonstrating its superiority

Method	Years	Traning Data	IC13	SVT	IIIT5K	IC15	SVT-P	CUTE80
CRNN [30]	2017	90K	86.7	80.8	78.2	–	–	–
FocusAtten [3]	2017	90K+ST	93.3	85.9	87.4	70.6	–	–
AON [4]	2018	90K+ST	–	82.8	87.0	68.2	73.0	76.8
ASTER [32]	2018	90K+ST	91.8	89.5	93.4	76.1	78.5	79.5
ESIR [45]	2019	90K+ST	91.3	90.2	93.3	76.9	79.6	83.3
SAR [16]	2019	90K+ST	91.0	84.5	91.5	69.2	76.4	83.3
2D-Attention [23]	2019	90K+ST	92.7	90.1	94.0	76.3	82.3	86.8
MaskTextSpotter [18]	2019	90K+ST	95.3	90.6	93.9	77.3	82.2	87.8
NRTR [29]	2019	90K+ST	95.8	91.5	90.1	79.4	86.6	80.9
SE-ASTER [27]	2020	90K+ST	92.8	89.6	93.8	80.0	81.4	83.6
Textscanner [35]	2020	90K+ST	92.9	90.1	93.9	79.4	84.3	83.3
DAN [38]	2020	90K+ST	93.9	89.2	94.3	74.5	80.0	84.4
RobustScanner [44]	2020	90K+ST	94.8	88.1	95.3	77.1	79.5	90.3
SRN [43]	2020	90K+ST	95.5	91.5	94.8	82.7	85.1	87.8
Pren2D [41]	2021	90K+ST+Real	96.4	94	95.6	83	87.6	<b>91.7</b>
JVSR [2]	2021	90K+ST	95.5	92.2	95.2	84.0	85.7	89.7
FTO [39]	2021	90K+ST	95.7	91.7	95.8	83.7	86.0	88.5
ABInet [6]	2021	90K+ST	97.4	93.5	96.2	86	89.3	89.2
CDistNet (Ours)	–	90K+ST	<b>97.67</b>	<b>93.82</b>	<b>96.57</b>	<b>86.25</b>	<b>89.77</b>	89.58

Table 7. Accuracy comparison with existing methods.

in recognizing difficult text. For both IC15 and SVT-P, accuracy improvements ranging from over 2 to 10 percents are observed for most competitors. CDistNet also outperforms other position-related methods [35, 44] by large margins on nearly all the datasets except for RobustScanner in CUTE80, indicating the effectiveness of the proposed positional utilization. It is also observed that CDistNet does not exhibit advantage in CUTE80, which recognizes character feature by position information. Therefore, methods (e.g., RobustScanner [44], JVSR [2]) good at capturing rich semantic clues perform well on CUTE80 in general. But their advantages cannot be retained for other datasets that exhibit different characteristics. In contrast, CDistNet consistently ranks top-tier. It perceives fine-grained distance information from both visual and semantic domains thus better handle challenges from different aspects.

## 5. Conclusion

Targeting to improve the accuracy of scene text recognition especially in extreme irregular text, we have presented the MDCDP module which utilizes positional feature to *query* both visual and semantic features within the attention-based encoder-decoder framework. It is conducive to learning a joint representation delineating character distance in both visual and semantic domains. Accordingly, CDistNet has been developed based on the MDCDP module for text recognition. We have carried out extensive experiments on eight datasets that successfully validate our



Figure 8. Good cases of CDistNet. Pred and GT denote the predicted result and ground-truth, respectively. Red color means incorrectly recognized characters. Below defined similarly.



Figure 9. Bad cases of CDistNet.

proposal. The result on augmented datasets shows larger accuracy margin is observed as the severity of deformation increases. While ablation studies demonstrate the effect of each proposed component. CDistNet reports state-of-the-

art accuracy when compared with existing methods on six standard benchmarks. In addition, the visualization experiments also basically verify that superior attention localization are obtained in both visual and semantic domains.

## References

- [1] Jeonghun Baek, Geewook Kim, Junyeop Lee, Sungrae Park, Dongyo Han, Sangdoo Yun, Seong Joon Oh, and Hwalsuk Lee. What is wrong with scene text recognition model comparisons? dataset and model analysis. In *International Conference on Computer Vision*, 2019. [1](#), [2](#), [4](#), [5](#)
- [2] Ayan Kumar Bhunia, Aneeshan Sain, Amandeep Kumar, Shuvrozit Ghose, Pinaki Nath Chowdhury, and Yi-Zhe Song. Joint visual semantic reasoning: Multi-stage decoder for text recognition. *ICCV*, 2021. [2](#), [8](#)
- [3] Zhanzhan Cheng, Fan Bai, Yunlu Xu, Gang Zheng, Shiliang Pu, and Shuigeng Zhou. Focusing attention: Towards accurate text recognition in natural images. In *Proceedings of the IEEE international conference on computer vision*, pages 5076–5084, 2017. [2](#), [3](#), [8](#)
- [4] Zhanzhan Cheng, Yangliu Xu, Fan Bai, Yi Niu, Shiliang Pu, and Shuigeng Zhou. Aon: Towards arbitrarily-oriented text recognition. In *Proceedings of the IEEE Conference on Computer Vision and Pattern Recognition*, pages 5571–5579, 2018. [2](#), [8](#)
- [5] Jacob Devlin, Ming-Wei Chang, Kenton Lee, and Kristina Toutanova. Bert: Pre-training of deep bidirectional transformers for language understanding. In *NAACL-HLT*, 2019. [3](#)
- [6] Shancheng Fang, Hongtao Xie, Yuxin Wang, Zhendong Mao, and Yongdong Zhang. Read like humans: Autonomous, bidirectional and iterative language modeling for scene text recognition. 2021. [1](#), [2](#), [3](#), [4](#), [5](#), [6](#), [8](#)
- [7] Ankush Gupta, Andrea Vedaldi, and Andrew Zisserman. Synthetic data for text localisation in natural images. In *Proceedings of the IEEE conference on computer vision and pattern recognition*, pages 2315–2324, 2016. [5](#)
- [8] Pan He, Weilin Huang, Yu Qiao, Chen Change Loy, and Xiaou Tang. Reading scene text in deep convolutional sequences. In *Thirtytieth AAAI conference on artificial intelligence*, 2016. [2](#)
- [9] Wenyang Hu, Xiaocong Cai, Jun Hou, Shuai Yi, and Zhiping Lin. Gtc: Guided training of ctc towards efficient and accurate scene text recognition. In *Proceedings of the AAAI Conference on Artificial Intelligence*, volume 34, pages 11005–11012, 2020. [2](#)
- [10] Max Jaderberg, Karen Simonyan, Andrea Vedaldi, and Andrew Zisserman. Synthetic data and artificial neural networks for natural scene text recognition. In *Workshop on Deep Learning, NIPS*, 2014. [5](#)
- [11] Max Jaderberg, Karen Simonyan, Andrew Zisserman, et al. Spatial transformer networks. *Advances in neural information processing systems*, 28:2017–2025, 2015. [3](#)
- [12] Dimosthenis Karatzas, Lluis Gomez-Bigorda, Anguelos Nicolaou, Suman Ghosh, Andrew Bagdanov, Masakazu Iwamura, Jiri Matas, Lukas Neumann, Vijay Ramaseshan Chandrasekhar, Shijian Lu, et al. Icdar 2015 competition on robust reading. In *2015 13th International Conference on Document Analysis and Recognition*, pages 1156–1160, 2015. [5](#)
- [13] Dimosthenis Karatzas, Faisal Shafait, Seiichi Uchida, Masakazu Iwamura, Lluis Gomez i Bigorda, Sergi Robles Mestre, Joan Mas, David Fernandez Mota, Jon Almazan Almazan, and Lluis Pere De Las Heras. Icdar 2013 robust reading competition. In *2013 12th International Conference on Document Analysis and Recognition*, pages 1484–1493, 2013. [5](#)
- [14] Zhenzhong Lan, Mingda Chen, Sebastian Goodman, Kevin Gimpel, Piyush Sharma, and Radu Soricut. Albert: A lite bert for self-supervised learning of language representations. *arXiv preprint arXiv:1909.11942*, 2019. [3](#)
- [15] Chen-Yu Lee and Simon Osindero. Recursive recurrent nets with attention modeling for ocr in the wild. In *Proceedings of the IEEE Conference on Computer Vision and Pattern Recognition*, pages 2231–2239, 2016. [1](#), [2](#)
- [16] Hui Li, Peng Wang, Chunhua Shen, and Guyu Zhang. Show, attend and read: A simple and strong baseline for irregular text recognition. In *Proceedings of the AAAI Conference on Artificial Intelligence*, volume 33, pages 8610–8617, 2019. [3](#), [4](#), [8](#)
- [17] Yi Li, Haozhi Qi, Jifeng Dai, Xiangyang Ji, and Yichen Wei. Fully convolutional instance-aware semantic segmentation. In *Proceedings of the IEEE conference on computer vision and pattern recognition*, pages 2359–2367, 2017. [2](#)
- [18] M. Liao, P. Lyu, M. He, C. Yao, W. Wu, and X. Bai. Mask textspotter: An end-to-end trainable neural network for spotting text with arbitrary shapes. *IEEE Transactions on Pattern Analysis and Machine Intelligence*, 43(2):532–548, 2019. [8](#)
- [19] Minghui Liao, Jian Zhang, Zhaoyi Wan, Fengming Xie, Jianjun Liang, Pengyuan Lyu, Cong Yao, and Xiang Bai. Scene text recognition from two-dimensional perspective. In *Proceedings of the AAAI Conference on Artificial Intelligence*, volume 33, pages 8714–8721, 2019. [2](#), [3](#)
- [20] Wei Liu, Chao Feng Chen, and Kwan-Yee K Wong. Charnet: A character-aware neural network for distorted scene text recognition. In *Thirty-Second AAAI Conference on Artificial Intelligence*, 2018. [2](#)
- [21] Canjie Luo, Yuanzhi Zhu, Lianwen Jin, and Yongpan Wang. Learn to augment: Joint data augmentation and network optimization for text recognition. In *Proceedings of the IEEE/CVF Conference on Computer Vision and Pattern Recognition*, pages 13746–13755, 2020. [5](#)
- [22] Pengyuan Lyu, Minghui Liao, Cong Yao, Wenhao Wu, and Xiang Bai. Mask textspotter: An end-to-end trainable neural network for spotting text with arbitrary shapes. In *Proceedings of the European Conference on Computer Vision*, pages 67–83, 2018. [2](#)
- [23] Pengyuan Lyu, Zhicheng Yang, Xinhang Leng, Xiaojun Wu, Ruiyu Li, and Xiaoyong Shen. 2d attentional irregular scene text recognizer. *arXiv preprint arXiv:1906.05708*, 2019. [3](#), [8](#)
- [24] Anand Mishra, Kartikey Alahari, and CV Jawahar. Scene text recognition using higher order language priors. In *British Machine Vision Conference*, 2012. [5](#)
- [25] Nguyen Nguyen, Thu Nguyen, Vinh Tran, Minh-Triet Tran, Thanh Duc Ngo, Thien Huu Nguyen, and Minh Hoai.

Dictionary-guided scene text recognition. In *Proceedings of the IEEE/CVF Conference on Computer Vision and Pattern Recognition*, pages 7383–7392, 2021. 2

[26] Trung Quy Phan, Palaiahankote Shivakumara, Shangxuan Tian, and Chew Lim Tan. Recognizing text with perspective distortion in natural scenes. In *Proceedings of the IEEE International Conference on Computer Vision*, pages 569–576, 2013. 5

[27] Zhi Qiao, Yu Zhou, Dongbao Yang, Yucan Zhou, and Weiping Wang. Seed: Semantics enhanced encoder-decoder framework for scene text recognition. In *2020 IEEE/CVF Conference on Computer Vision and Pattern Recognition*, pages 13525–13534. IEEE, 2020. 2, 3, 8

[28] Anhar Risnumawan, Palaiahankote Shivakumara, Chee Seng Chan, and Chew Lim Tan. A robust arbitrary text detection system for natural scene images. *Expert Systems with Applications*, 41(18):8027–8048, 2014. 5

[29] Fenfen Sheng, Zheneng Chen, and Bo Xu. Nrtr: A no-recurrence sequence-to-sequence model for scene text recognition. In *2019 International Conference on Document Analysis and Recognition*, pages 781–786. IEEE, 2019. 1, 2, 3, 4, 6, 7, 8

[30] Baoguang Shi, Xiang Bai, and Cong Yao. An end-to-end trainable neural network for image-based sequence recognition and its application to scene text recognition. *IEEE Trans. Pattern Anal. Mach. Intell.*, 39(11):2298–2304, 2017. 1, 2, 8

[31] Baoguang Shi, Xinggang Wang, Pengyuan Lyu, Cong Yao, and Xiang Bai. Robust scene text recognition with automatic rectification. In *Proceedings of the IEEE conference on computer vision and pattern recognition*, pages 4168–4176, 2016. 3

[32] Baoguang Shi, Mingkun Yang, Xinggang Wang, Pengyuan Lyu, Cong Yao, and Xiang Bai. Aster: An attentional scene text recognizer with flexible rectification. *IEEE transactions on pattern analysis and machine intelligence*, 41(9):2035–2048, 2018. 2, 3, 4, 8

[33] Bolan Su and Shijian Lu. Accurate recognition of words in scenes without character segmentation using recurrent neural network. *Pattern Recognition*, 63:397–405, 2017. 2

[34] Ashish Vaswani, Noam Shazeer, Niki Parmar, Jakob Uszkoreit, Llion Jones, Aidan N Gomez, Łukasz Kaiser, and Illia Polosukhin. Attention is all you need. In *NIPS*, pages 5998–6008, 2017. 2, 3, 4, 6

[35] Zhaoyi Wan, Minghang He, Haoran Chen, Xiang Bai, and Cong Yao. Textscanner: Reading characters in order for robust scene text recognition. In *Proceedings of the AAAI Conference on Artificial Intelligence*, volume 34, pages 12120–12127, 2020. 2, 3, 8

[36] Kai Wang, Boris Babenko, and Serge Belongie. End-to-end scene text recognition. In *2011 International Conference on Computer Vision*, pages 1457–1464, 2011. 5

[37] Peng Wang, Lu Yang, Hui Li, Yuyan Deng, Chunhua Shen, and Yanning Zhang. A simple and robust convolutional-attention network for irregular text recognition. *arXiv preprint arXiv:1904.01375*, 6:2, 2019. 1, 3

[38] Tianwei Wang, Yuanzhi Zhu, Lianwen Jin, Canjie Luo, Xiaoxue Chen, Yaqiang Wu, Qianying Wang, and Mingxiang Cai. Decoupled attention network for text recognition. In *Proceedings of the AAAI Conference on Artificial Intelligence*, volume 34, pages 12216–12224, 2020. 2, 4, 8

[39] Yuxin Wang, Hongtao Xie, Shancheng Fang, Jing Wang, Shenggao Zhu, and Yongdong Zhang. From two to one: A new scene text recognizer with visual language modeling network. *ICCV*, 2021. 3, 8

[40] Linjie Xing, Zhi Tian, Weilin Huang, and Matthew R Scott. Convolutional character networks. In *Proceedings of the IEEE/CVF International Conference on Computer Vision*, pages 9126–9136, 2019. 2

[41] Ruijie Yan, Liangrui Peng, Shanyu Xiao, and Gang Yao. Primitive representation learning for scene text recognition. In *Proceedings of the IEEE/CVF Conference on Computer Vision and Pattern Recognition*, pages 284–293, 2021. 8

[42] Mingkun Yang, Yushuo Guan, Minghui Liao, Xin He, Kaigui Bian, Song Bai, Cong Yao, and Xiang Bai. Symmetry-constrained rectification network for scene text recognition. In *Proceedings of the IEEE/CVF International Conference on Computer Vision*, pages 9147–9156, 2019. 3

[43] Deli Yu, Xuan Li, Chengquan Zhang, Tao Liu, Junyu Han, Jingtuo Liu, and Errui Ding. Towards accurate scene text recognition with semantic reasoning networks. In *Proceedings of the IEEE/CVF Conference on Computer Vision and Pattern Recognition*, pages 12113–12122, 2020. 1, 2, 4, 5, 6, 8

[44] Xiaoyu Yue, Zhanghui Kuang, Chenhao Lin, Hongbin Sun, and Wayne Zhang. Robustscanner: Dynamically enhancing positional clues for robust text recognition. In *European Conference on Computer Vision*, pages 135–151. Springer, 2020. 2, 3, 4, 5, 6, 7, 8

[45] Fangneng Zhan and Shijian Lu. Esir: End-to-end scene text recognition via iterative image rectification. In *Proceedings of the IEEE/CVF Conference on Computer Vision and Pattern Recognition*, pages 2059–2068, 2019. 3, 8